

Supporting information

In-situ anchoring of Zn-doped ZIF-67 on carboxymethylated bacterial cellulose for effective indigo carmine capture

Tian Mai,^a Pei-Lin Wang,^a Qi Yuan,^a Chang Ma,^a Ming-Guo Ma^{*a}

^aResearch Center of Biomass Clean Utilization, Beijing Key Laboratory of Lignocellulosic Chemistry, College of Materials Science and Technology, Beijing Forestry University, Beijing 100083, P. R. China.

1. Supplementary Tables

Table S1. Specific surface area of as-prepared materials.

	Pure BC	ZCMBC composite films	ZnZIF-67
BET surface area ($\text{m}^2 \cdot \text{g}^{-1}$)	1.8	66.9	1590.0
Langmuir surface area ($\text{m}^2 \cdot \text{g}^{-1}$)	9.5	816.9	1915.2

Table S2. Adsorption kinetic study model parameters for IC- adsorption on ZCMBC composite films.

	K ₁	K ₂	q _{e,cal}	R ²
Pseudo-first-order model	0.34	-	15.1	0.98
Pseudo-second-order model	-	0.037	16.1	0.99

Table S3. Adsorption isotherm model parameters for IC- adsorption on ZCMBC composite films.

	K _L	K _F	q _{m,cal}	n	R ²
Langmuir adsorption isotherm	0.0016	-	264.6	-	0.99
Freundlich adsorption isotherm	-	1.93	-	0.65	0.96

Table S4. Thermodynamics parameters for the adsorption of IC- on ZCMBC composite films.

T (K)	ΔG ⁰ (kJ·mol ⁻¹)	ΔH ⁰ (kJ·mol ⁻¹)	ΔS ⁰ (kJ·mol ⁻¹ ·K ⁻¹)
303.15	-5.7		
313.15	-5.1	-15.5	0.03
323.15	-5.0		

Table S5. Comparison of the dye removal efficiency of dyes with other metal-organic frameworks and nanocellulose composites adsorbents.

Materials	Dyes	Initial dye concentration	Removal efficiency	Ref
ZIF-8/OCBs	Methyl orange	50 ppm	84.0%	1
HKUST-1/OCBs			55.0%	
MIL-100(Fe)@BC	Rhodamine B	10 ppm	85.0%	2
ZIF-67@CA	Methyl orange	5 ppm	96.4%	3
ZCMBC	Indigo carmine	50 ppm	98.7%	This work

Table S6. The models and equations mentioned in this work.

	Equation	Ref
Adsorption capacity at special time (q_t , $\text{mg}\cdot\text{g}^{-1}$)	$q_t = \frac{(C_0 - C_t)V}{m}$	-
Equilibrium adsorption capacity (q_e , $\text{mg}\cdot\text{g}^{-1}$)	$q_e = \frac{(C_0 - C_e)V}{m}$	-
Removal efficiency	$R\% = \frac{C_e - C_0}{C_0} \times 100$	-
Loading rate	$L\% = \frac{m_{ZCMBC} - m_{CMBC}}{m_{ZnZIF-67} - m_{CMBC}} \times 100$	4
Pseudo-first-order model	$\ln(q_e - q_t) = \ln q_e - k_1 t$	5
Pseudo-second-order model	$\frac{t}{q_t} = \frac{1}{k_2 q_e^2} + \frac{t}{q_e}$	6
Langmuir adsorption isotherm	$q_e = \frac{q_m K_L C_e}{1 + K_L C_e}$	7
Freundlich adsorption isotherm	$q_e = K_F C_e^n$ $k_D = \frac{q_e}{C_e}$	8
Adsorption thermodynamic formulas	$\Delta G^0 = -RT \ln k_D$ $\ln k_D = \frac{\Delta S^0}{R} - \frac{\Delta H^0}{RT}$	9

Where m (g) is the dry mass of ZCMBC composite film. V is the volume of the dye solution, C_0 ($\text{mg}\cdot\text{L}^{-1}$) is the initial concentration of dye, and C_e ($\text{mg}\cdot\text{L}^{-1}$) is the concentration of dye in solution

when the adsorption reaches equilibrium. L% represents the loading rate of ZnZIF-67, and the m_{ZCMBC} , m_{CMBC} , $m_{ZnZIF-67}$ represent the weight residues of the ZCMBC, CMBC and ZnZIF-67, respectively. $q_t(\text{mg}\cdot\text{g}^{-1})$ is the adsorption capacity at time t. $C_t (\text{mg}\cdot\text{L}^{-1})$ is the concentration of dye at time t; Where $k_1 (\text{min}^{-1})$ and $k_2 (\text{g}\cdot\text{mg}^{-1}\cdot\text{min}^{-1})$ is the adsorption rate coefficient of pseudo-first order model and pseudo-second order model. For adsorption isotherm model, q_m is the max adsorption capacity. K_L is Langmuir constant ($\text{L}\cdot\text{mg}^{-1}$); R_L value is dimensionless separation factor, reflecting the favourability of adsorption. When $R_L > 1$, it is not conducive to adsorption, and when $0 < R_L < 1$, adsorption is easy to occur. K_F is Freundlich isotherm constant ($\text{L}\cdot\text{g}^{-1}$), and n is Freundlich exponent. For adsorption thermodynamic formulas, k_D is the equilibrium partition constant; ΔG^0 ($\text{kJ}\cdot\text{mol}^{-1}$) is Gibbs free energy, and ΔH^0 ($\text{kJ}\cdot\text{mol}^{-1}$) is enthalpy change and ΔS^0 ($\text{kJ}\cdot\text{mol}^{-1}\cdot\text{K}^{-1}$) is entropy change; R ($8.314 \text{ J}\cdot\text{mol}^{-1}\cdot\text{K}^{-1}$) is the universal gas constant; T (K) is the adsorption temperature.

2. Supplementary Figures

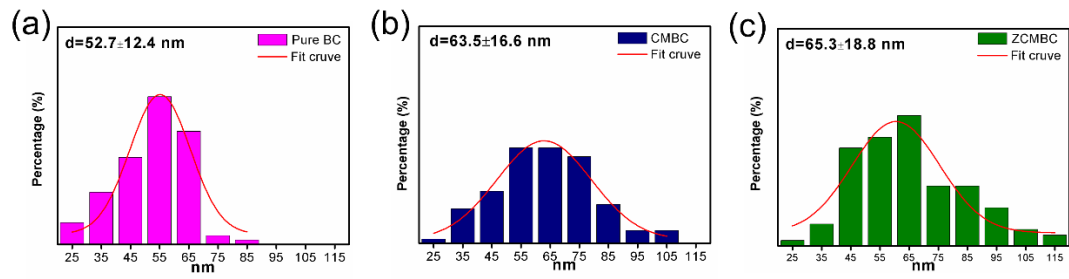


Fig. S1. The diameter distribution of pure BC (a), CMBC (b), and ZCMBC composite films (c), respectively.

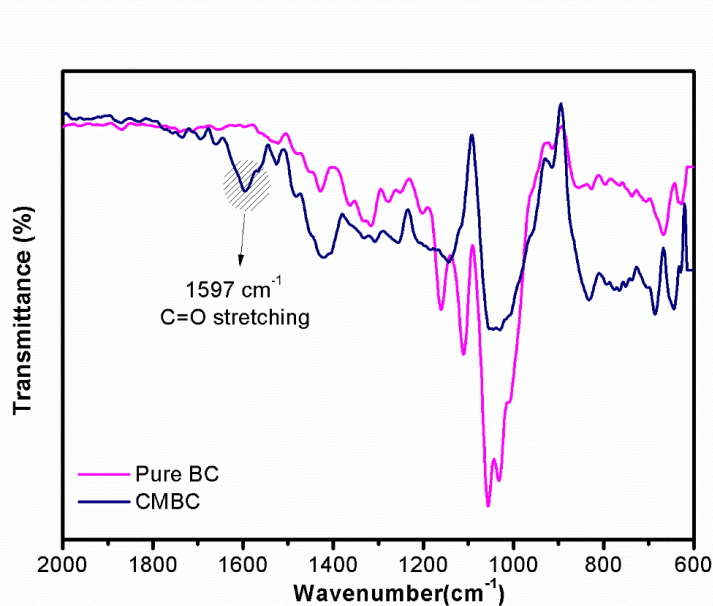


Fig. S2. The FTIR spectra of pure BC and CMBC.

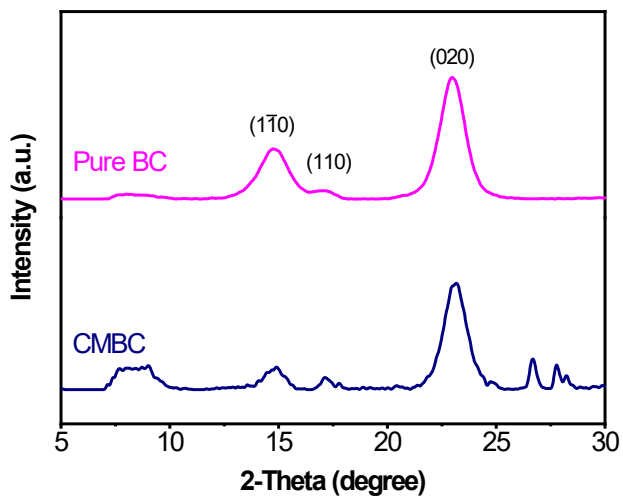


Fig. S3. The XRD spectra of pure BC and CMBC.

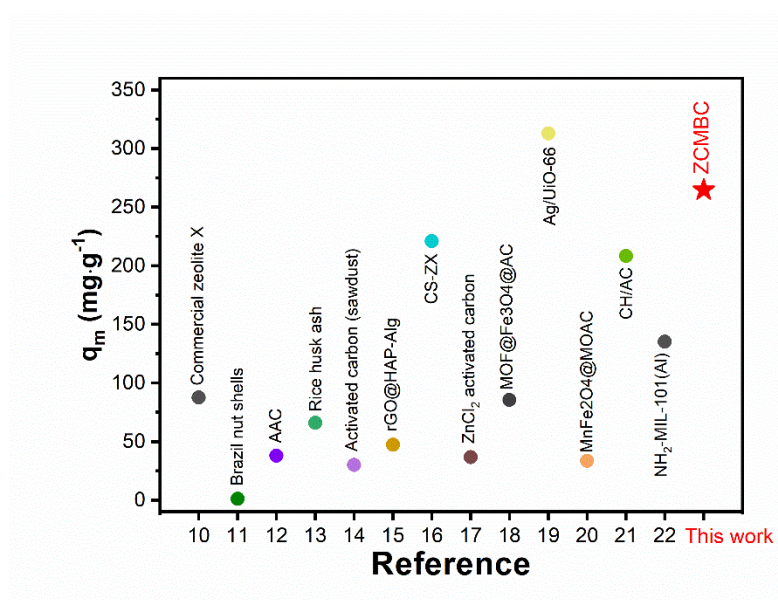


Fig. S4. Comparison of the IC- adsorption capacities of ZCMBC composite films and other

adsorbents.¹⁰⁻²²

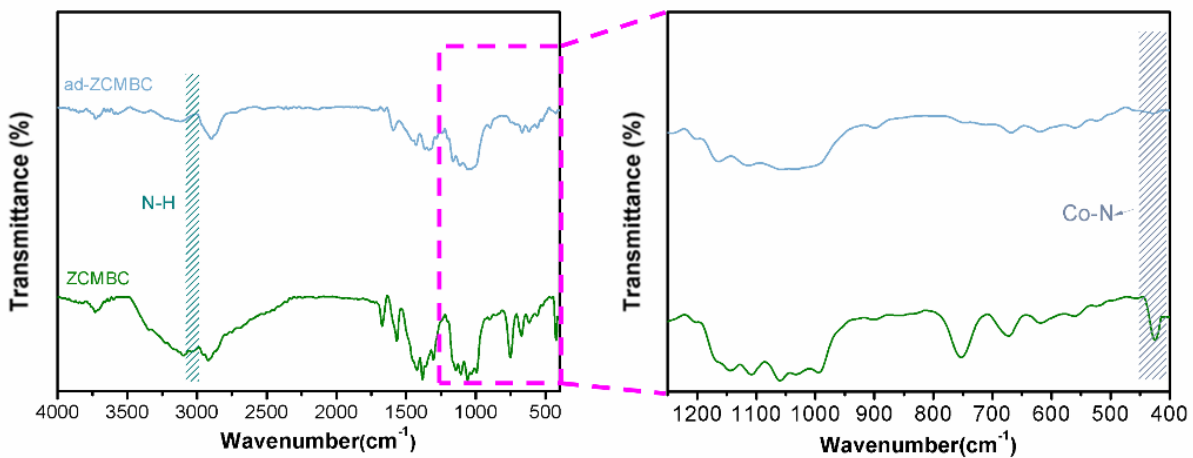


Fig. S5. FTIR spectra of ZCMBC composite films before and after adsorption of IC⁻.

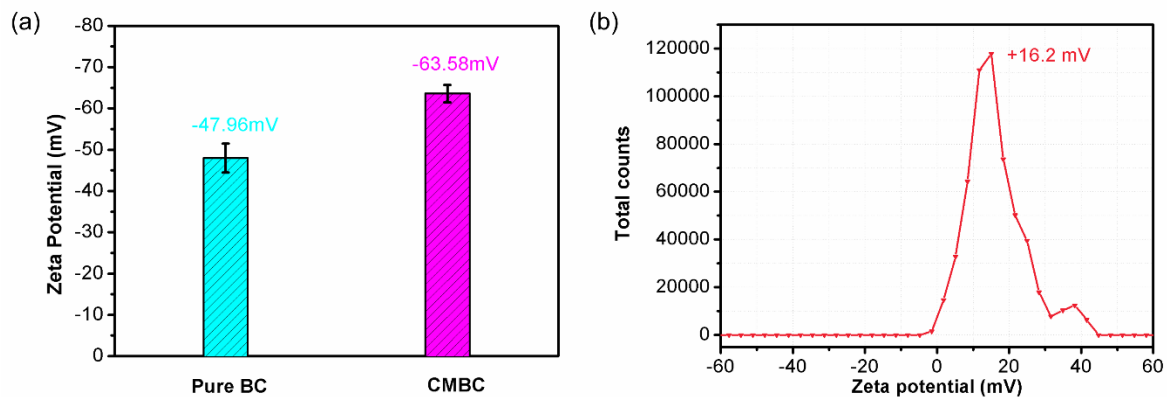


Fig. S6. Solid Zeta-potential measurement of pure BC, CMBC (a) and powder Zeta-potential measurement of ZnZIF-67 (b) in water (pH=7), respectively.

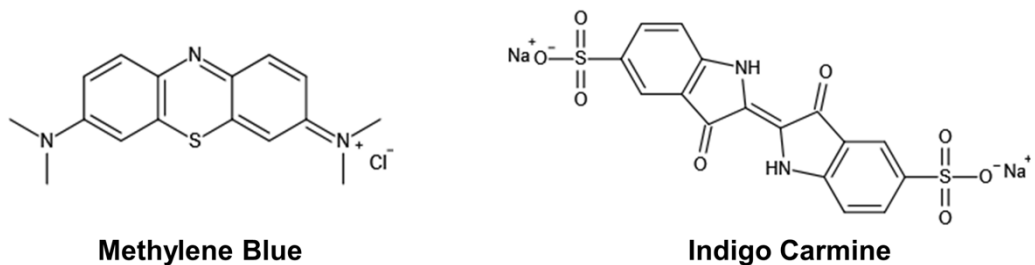


Fig. S7. Molecular structures of dyes used.

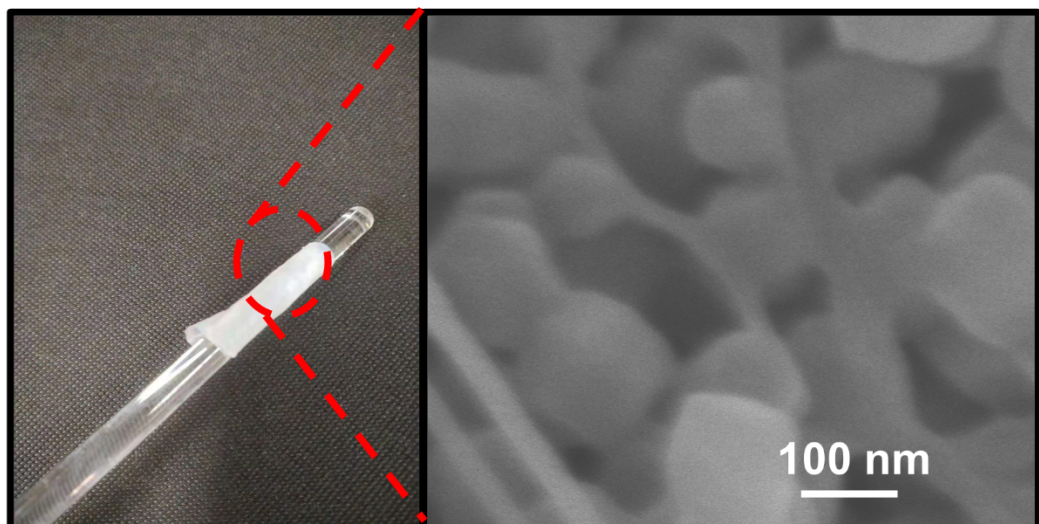


Fig. S8. The digital photograph and SEM image of ZCMBC-8 composite films.

Supplementary References

1. C. Duan, X. Meng, C. Liu, W. Lu, J. Liu, L. Dai, W. Wang, W. Zhao, C. Xiong and Y. Ni, *Carbohydr. Polym.*, 2019, **222**, 115042.
2. R. M. Ashour, A. F. Abdel-Magied, Q. Wu, R. T. Olsson and K. Forsberg, *Polymers*, 2020, **12**, 1104.
3. W. Song, M. Zhu, Y. Zhu, Y. Zhao, M. Yang, Z. Miao, H. Ren, Q. Ma and L. Qian, *Cellulose*, 2020, **27**, 2161-2172.
4. D. W. Li, X. J. Tian, Z. Q. Wang, Z. Guan, X. Q. Li, H. Qiao, H. Z. Ke, L. Luo and Q. F. Wei, *Chem. Eng. J.*, 2020, **383**, 123127.
5. Y.-d. Huang, *Powder Technol.*, 2018, **324**, 16-17.
6. K. V. Kumar, *J Hazard Mater*, 2006, **137**, 1538-1544.
7. B. Doshi, A. Ayati, B. Tanhaei, E. Repo and M. Sillanpaa, *Carbohydr Polym*, 2018, **197**, 586-597.
8. M. W. Donner, M. Arshad, A. Ullah and T. Siddique, *Sci Total Environ*, 2019, **647**, 1539-1546.
9. G. Chen, S. He, G. Shi, Y. Ma, C. Ruan, X. Jin, Q. Chen, X. Liu, H. Dai, X. Chen and D. Huang, *Chem. Eng. J.*, 2021, **423**, 130184.
10. S. Sivalingam and S. Sen, *Chemosphere*, 2018, **210**, 816-823.
11. S. M. de Oliveira Brito, H. M. Andrade, L. F. Soares and R. P. de Azevedo, *J Hazard Mater*, 2010, **174**, 84-92.
12. T. B. Gupta and D. H. Lataye, *J. Hazard. Toxic Radioact. Waste*, 2017, **21**, 04017013.
13. U. R. Lakshmi, V. C. Srivastava, I. D. Mall and D. H. Lataye, *J Environ Manage*, 2009, **90**, 710-720.
14. D. Sikdar, S. Goswami and P. Das, *Biomass Conversion and Biorefinery*, 2021, DOI: 10.1007/s13399-021-01385-1.
15. P. Sirajudheen, P. Karthikeyan, S. Vigneshwaran, C. B. M and S. Meenakshi, *Int J Biol Macromol*, 2021, **175**, 361-371.
16. A. Marotta, E. Luzzi, M. Salzano de Luna, P. Aprea, V. Ambrogi and G. Filippone, *Polymers (Basel)*, 2021, **13**, 1691.
17. M. Paredes-Laverde, M. Salamanca, J. D. Diaz-Corrales, E. Flórez, J. Silva-Agredo and R. A. Torres-Palma, *J. Environ. Chem. Eng.*, 2021, **9**, 105685.
18. R. Paz, H. Viltres, N. K. Gupta and C. Leyva, *J. Mol. Liq.*, 2021, **337**, 116578.
19. R. S. Salama, E.-S. M. El-Sayed, S. M. El-Bahy and F. S. Awad, *Colloid Surf. A-Physicochem. Eng. Asp.*, 2021, **626**, 127089.
20. P. Sirajudheen, P. Karthikeyan, K. Ramkumar, P. Nisheetha and S. Meenakshi, *J. Mol. Liq.*, 2021, **327**, 114829.
21. J. K. Fatombi, E. A. Idohou, S. A. Osseni, I. Agani, D. Neumeyer, M. Verelst, R. Mauricot and T. Aminou, *Fiber. Polym.*, 2019, **20**, 1820-1832.
22. H. Liu, L. Chen and J. Ding, *RSC Adv*, 2016, **6**, 48884-48895.